An Experimental and Multiphysics Simulations Study of *Clostridium carboxidivorans* sp. 624 for Acid and Alcohol Production in CO_2/H_2

Yong Wei Tiong[a, b, 1, *], Ashriel Yong[a, b, 1], Anjaiah Nalaparaju[c, 1, *], Hoang-Huy Nguyen[c, 1], Li Quan Koh[a], Roong Jien Wong[a], Ron Tau Yee Lim[a], Dave Siak-Wei Ow[d], Jia Zhang[c], Van Bo Nguyen[c], Fong Tian Wong[a, b, e, *], Yee Hwee Lim[a, b, f, *]

[a]Institute of Sustainability for Chemicals, Energy and Environment (ISCE[2]), Agency for Science, Technology and Research (A*STAR), 1 Pesek Road, Jurong Island, Singapore 627833, Republic of Singapore

[b]Singapore Integrative Biosystems and Engineering Research (SIBER), Agency for Science, Technology and Research (A*STAR), 20 Biopolis Way, #08-01 Centros, Singapore 138668, Republic of Singapore

[c]Institute of High Performance Computing (IHPC), Agency for Science, Technology and Research (A*STAR), 1 Fusionopolis Way, #16-16 Connexis North, Singapore 138632, Republic of Singapore

[d]Bioprocessing Technology Institute (BTI), Agency for Science, Technology and Research (A*STAR), 20 Biopolis Way, #06-01 Centros, Singapore 138668, Republic of Singapore

[e]Institute of Molecular and Cell Biology (IMCB), Agency for Science, Technology and Research (A*STAR), 61 Biopolis Drive, #07-06 Proteos, Singapore 138673, Republic of Singapore

[f]Synthetic Biology Translational Research Program, Yong Loo Lin School of Medicine, National University of Singapore, 10 Medical Drive, Singapore 117597, Republic of Singapore

[1]These authors contributed equally to this work.

*Co-corresponding authors:

Institute of Sustainability for Chemicals, Energy and Environment (ISCE[2]), Agency for Science, Technology and Research (A*STAR), 1 Pesek Road, Jurong Island, Singapore 627833, Republic of Singapore.

Email address:

lim_yee_hwee@isce2.a-star.edu.sg (Yee Hwee Lim),

wongft@imcb.a-star.edu.sg (Fong Tian Wong),

Tiong_Yong_Wei@isce2.a-star.edu.sg (Yong Wei Tiong)

Institute of High Performance Computing (IHPC), Agency for Science, Technology and Research (A*STAR), 1 Fusionopolis Way, #16-16 Connexis North, Singapore, 138632 Republic of Singapore.

Email address: Anjaiah_Nalaparaju@ihpc.a-star.edu.sg (Anjaiah Nalaparaju)

Abstract

Biotechnological advances in CO_2 utilization through gas fermentation offer a sustainable alternative to energy-intensive chemical processes. This study investigates and optimizes fermentation dynamics of *Clostridium carboxidivorans* sp. 624 for enhanced production of C_2–C_6 acids *via* combined experimental and computational methods. A systematic experimental evaluation of temperature and medium conditions, along with time-course analysis elucidates metabolic pathway regulation. Experimental optimisation, complemented by modelling, identified gas-liquid volumetric ratios $V_L/V_G = 4$ as optimal for maximizing longer-chain acids production, attributed to enhanced gas solubility and substrate bioavailability. Additionally, a hybrid model combining dynamic-kinetic model and computational fluid dynamics (CFD) successfully predict product formation. By capturing spatial inhomogeneities in gas-liquid interactions, the model also provides critical insights for optimizing fermentation performance and establishes a framework for improving process design parameters for CO_2/H_2 fermentation, paving the way for scalable and efficient CO_2-based bioprocesses.

Keywords: *Clostridium carboxidivorans*; CO_2 fermentation; Process optimization; Acid and alcohol selectivity; Dynamic-kinetic modelling; Computational fluid dynamics

1. Introduction

Since the Industrial Revolution, human activities have significantly raised atmospheric CO_2 concentrations, primarily due to the burning of fossil fuels. Consequently, CO_2 levels have increased from approximately 277 ppm in 1750 to 421 ppm in 2022, contributing to global climate change and its associated environmental impacts (Raganati and Ammendola, 2024). To mitigate emissions, the Paris Agreement targets a 50–100% reduction by 2030 and beyond (Dziejarski et al., 2023). Surrounded by this, biotechnological CO_2 utilization is emerging as a sustainable alternative to energy-intensive chemical catalysis (Liew et al., 2016), leveraging microorganisms to convert CO_2 into valuable bio-based products and advancing a circular economy (Ricci et al., 2021).

One promising approach is anaerobic CO_2 gas fermentation, in which clostridial acetogens utilize the Wood-Ljungdahl pathway (WLP), also known as the reductive acetyl-CoA pathway, to fix CO_2 (Acuña et al., 2024; Antonicelli et al., 2023; Ntagia et al., 2021). The resulting acetyl-CoA undergoes further metabolic reactions to produce organic acids and alcohols (Sun et al., 2019). This process occurs in two distinct phases: acidogenesis (organic acid production) and solventogenesis (conversion to alcohols), where CO_2 serves as the electron acceptor and H_2 as the donor, enabling CO_2 fixation and sustainable bioproduction (Mariën et al., 2024). Despite advancements in syngas fermentation using CO, CO_2, and H_2 (Doll et al., 2018; Fernández-Naveira et al., 2019; Phillips et al., 2015), CO_2/H_2 fermentation remains in the early stages of bioengineering, primarily yielding acetate (Molitor et al., 2019) and low ethanol titers (Heffernan et al., 2020). Expanding production to higher-value medium-chain C_4 and C_6 bio-based chemicals is essential for improving the economic feasibility of CO_2 fermentation (Thunuguntla et al., 2024).

Among acetogenic bacteria, *Clostridium carboxidivorans* sp. 624 is known for producing a wide range of C_2 to C_6 acids and alcohols, including acetate, butyrate, ethanol,

butanol, hexanoate, and hexanol, when utilizing syngas or CO-based feedstocks (Oh et al., 2022; Phillips et al., 2015). In syngas fermentation ($CO/H_2/CO_2$ [70/20/10]), this strain produced mainly ethanol (~3.00 g/L) and hexanol (0.94 g/L) (Phillips et al., 2015), while a different syngas mixture ($CO/H_2/CO_2$ [30/40/30]) yielded 4.32 g/L total alcohols, with hexanol (1.90 g/L) as the dominant product (Oh et al., 2022). However, research on pure CO_2/H_2 fermentation remains limited. A recent study employing Adaptive Laboratory Evolution (ALE) reported modest metabolite yields, including acetate (0.82 g/L), butyrate (0.38 g/L), and hexanoate (0.40 g/L), alongside low alcohol titers (0.23–0.27 g/L) under CO_2/H_2 fermentation (Antonicelli et al., 2023). These findings highlight challenges such as limited metabolite titers and variability in product distribution, underscoring the need for optimization in microbial pathways and fermentation parameters to enhance CO_2-based biomanufacturing. Importantly, CO_2/H_2 fermentation could also offer a promising direct utilization pathway for CO_2, without requirements of CO inputs.

In addition to experimental optimization, modelling and simulation can play a crucial role in optimizing bioprocesses by analyzing parameters *in silico*, minimizing trial-and-error experimentation, and accelerating process development. In C_1 gas fermentation by the clostridial microbiome, dynamic-kinetic model captures microbial metabolic pathways and integrates mass balance to generate time-dependent metabolite profiles. Computational tools, including dynamic simulations and computational fluid dynamics (CFD), assess mass transfer, which is critical in gas-to-liquid fermentation systems (Puiman et al., 2022). Modelling CO_2 and H_2 spatial distribution provides insights into their impact on microbial growth and metabolite production (Singh et al., 2024). Despite advancements in gas fermentation modelling, models specifically tailored for CO_2/H_2 fermentation in clostridial strains producing C_2-C_6 metabolites remained unstudied, with most studies focused on CO as the primary substrate (Ruggiero et al., 2022; Younesi et al., 2005).

Herein, this study systematically evaluates CO_2/H_2-based fermentation of *C. carboxidivorans* sp. 624 towards the production of C_2–C_6 acids and alcohols through a combined experimental and *in silico* approach. A time-course study examines the metabolic dynamics of C_2–C_6 acid and alcohol production, providing insights into pathway regulation and intermediate accumulation. Using the experimental data, an integrated model featuring a hybrid CFD simulation-first principles kinetic model was developed to predict product formation. By capturing spatial inhomogeneities in gas-liquid interactions, the model also provides critical insights for optimizing fermentation performance and establishes a framework for improving process design parameters for CO_2/H_2 fermentation, paving the way for scalable and efficient CO_2-based bioprocesses.

2. Materials and Methods

2.1 Microorganism and medium preparation

C. carboxidivorans sp. BAA-624 was purchased from American Type Culture Collection (ATCC, USA). The modified PETC medium was prepared by dissolving the following components per liter of deionized water: 0.10 g KCl, 0.20 g $MgSO_4 \cdot 7H_2O$, 0.80 g NaCl, 0.10 g KH_2PO_4, 0.02 g $CaCl_2 \cdot 2H_2O$, 1.00 g yeast extract, and 2.00 g $NaHCO_3$. Additionally, 10 mL of modified Wolfe's metals solution (Med 1788) and 10 mL of Wolfe's vitamin solution (MD-VS; Med 1019) were added to supplement the medium. Reinforced Clostridial Medium (RCM, Thermo Scientific™ Oxoid™ Reinforced Clostridial Medium) was prepared from a dehydrated powder (Thermo Scientific™ Oxoid™, catalog number CM0149B) according to the manufacturer's instructions.

Fermentation was conducted in 30 mL sterilized serum bottles, each containing 15 mL of PETC/RCM medium and 15 mL of headspace. The headspace was flushed for 1 minute with a CO_2/H_2 gas mixture (20/80), after which the pressure was equilibrated to 150 kPa (1.5 bar)

with the same gas. To maintain consistent gas substrate availability, the headspace of each culture bottle was replenished daily by flushing with fresh CO_2/H_2 (20/80) for 1 minute and equilibrated to 150 kPa. Fermentation was carried out at 25°C, 30°C, and 37°C under mild agitation at 200 rpm using an orbital shaker (Yih Der, LM-570RD). Control cultures were prepared by sparging with N_2 gas following the same procedure as the experimental conditions, which involved sparging for 1 minute and equilibrating to 150 kPa. N_2 gas controls are presented in **Fig.1-2** and **Fig S1-S2**. All data are reported as mean values from triplicate experiments ± standard error of the mean.

2.2 Analytical methods

Biomass analysis: The samples from fermentation were analysed with a multimode microplate reader (Thermo Scientific™ Varioskan™ LUX, USA) for optical density (OD=800nm) measurements, and a correlation factor was used to obtain cell dry weight (CDW) concentrations. To obtain CDW conversion factor, a sample volume with known OD was pelletised and supernatant discarded. The pellet was dried at 60 °C for 48 hours followed by gravimetric analysis to determine CDW% per volume. Maximum specific growth rates were estimated by applying a non-linear regression to the experimentally obtained data for CDW concentrations.

Metabolites analysis: C_2-C_6 metabolites (ethanol, butanol, hexanol, acetate, butyrate, and hexanoate) from fermentation were analysed using a gas chromatography (GC) (Agilent 6890N GC, Agilent Technologies, USA) with a flame ionization detector (FID) and fused silica capillary column (DB-WAX 60 m length x 0.53 mm diameter x 1.00 µm film thickness). Helium was used as the carrier gas. The initial oven temperature was set at 35 ^{o}C with a holding time of 4 min, and then gradually increased to 220 ^{o}C at a rate of 10 ^{o}C/min, and held at the final temperature for 6 min. The injector and detector temperatures were both set to 300°C. Prior to GC analysis, the sample was centrifuged, and the supernatant was filter through a 0.22

μm filter. A 0.50 mL portion of the supernatant was then acidified with 0.02 mL of 0.60 N HCl before proceeding with the analysis. Production yields of the C_2-C_6 metabolites reported herein have been referenced to 0 at t = 0 hour.

2.3 Kinetic model of microbial reactions

The biochemical reactions involved in the conversion of CO_2/H_2 to C_2-C_6 acids and alcohols by *C. carboxidivorans* sp. 624 during both the acetogenic and solventogenic phases, via the WLP and reverse *β*-oxidation, are presented in equations below (**eq. 1-6**).

Acetogenic phase:

$$4H_2 + 2CO_2 \rightarrow CH_3COOH + 2H_2O \quad (1)$$

$$CH_3COOH + 6H_2 + 2CO_2 \rightarrow C_3H_7COOH + 4H_2O \quad (2)$$

$$C_3H_7COOH + 6H_2 + 2CO_2 \rightarrow C_5H_{11}COOH + 4H_2O \quad (3)$$

Solventogenic phase:

$$CH_3COOH + 2H_2 \rightarrow C_2H_5OH + H_2O \quad (4)$$

$$C_3H_7COOH + 2H_2 \rightarrow C_4H_9OH + H_2O \quad (5)$$

$$C_5H_{11}COOH + 4H_2 \rightarrow C_6H_{13}OH + H_2O \quad (6)$$

To describe the rates of acid production (q_{AC}, q_{BA}, and q_{HA}), modified Monod equations that incorporate the inhibition effects of non-substrate fatty acids were applied (**eq. 7-9**). The conversion rate of acids in the presence of H_2 to produce alcohols (q_E, q_B and q_H) were expressed as Monod kinetic for substrates (**eq. 10-12**).

$$q_{Ac} = \mu_{Ac} \frac{C_{H2}}{K_{H2}^{i}+C_{H2}} \frac{K_{Ac}}{K_{Ac}+C_{Ac}} \frac{K_{BA}}{K_{BA}+C_{BA}} \quad (7)$$

$$q_{BA} = \mu_{BA} \frac{C_{H2}}{K_{H2}^{i}+C_{H2}} \frac{C_{Ac}}{K_{Ac}+C_{Ac}} \frac{K_{BA}}{K_{BA}+C_{BA}} \quad (8)$$

$$q_{HA} = \mu_{HA} \frac{C_{H2}}{K_{H2}^{i}+C_{H2}} \frac{C_{BA}}{K_{BA}+C_{BA}} \frac{K_{AC}}{K_{AC}+C_{AC}} \quad (9)$$

$$q_E = \mu_E \frac{C_{H2}}{K_{H2}^j + C_{H2}} \frac{C_{UAC}}{K_{UAC} + C_{UAc}} \quad (10)$$

$$q_B = \mu_B \frac{C_{H2}}{K_{H2}^j + C_{H2}} \frac{C_{UBA}}{K_{UBA} + C_{UBA}} \quad (11)$$

$$q_H = \mu_H \frac{C_{H2}}{K_{H2}^j + C_{H2}} \frac{C_{UHA}}{K_{UHA} + C_{UHA}} \quad (12)$$

where μ_i (i=AC, BA, HA) are the maximum uptake rates of biomass for acids production, μ_j (j=E, B, H) are the maximum production rates of alcohols, K_{H2}^i,K_i (i=AC, BA, HA) are affinity constants for biomass, K_{H2}^j,K_m *(m=UAC, UBA, UHA)* are saturation constants of H_2, undissociated acids. C_n (n=AC, BA, HA, H2, UAC, UBA, UHA) concentration in liquid phase. (Abbreviation: AC-acetate, BA-butyrate, HA-hexanoate, E-ethanol, B-butanol, and H-hexanol)

The component mass balance equations for the gas and liquid phases are provided in **Table S1**. These first-principles 0D dynamic-kinetic model equations were numerically solved to generate time profiles for product formation, and kinetic model parameters were estimated to achieve optimal representation of the experimental data. The mass transfer coefficient (K_La) and Henry's constant (K_H) for H_2 were obtained from literature sources (Manna et al., 2024).

2.4 CFD simulation for gas fermentation in serum bottle

To model multiphase flows in bioreactors, the Eulerian-Eulerian solver for multiple incompressible fluid phases in OpenFOAM (Weller et al., 1998) was employed for transient simulations. This solver treats each phase as a continuous fluid with distinct volume fractions, making it suitable for modelling and analysing complex fluid interactions in scenarios such as gas-liquid-cell flows and bubbly flows. Given the critical role of mass transfer in controlled aeration and microbial metabolism, the Higbie mass transfer model was integrated into the OpenFOAM framework, demonstrating superior accuracy compared to the existing spherical

and Frössling gas-liquid mass transfer models (Mast et al., 2024). The detailed equations for this implementation were provided in **Eq. 13–16**.

In the current simulation framework, the biological model serves as a phenomenological representation of the complex metabolic processes of a specific microorganism. To enhance computational efficiency, the reaction model was simplified while retaining key kinetic phenomena necessary for quantitative experimental validation. This reduced-order model was then integrated with the multiphase flow model to capture essential biochemical interactions. The evolution of microbial and species concentrations follows the kinetic model detailed in **Table S1**. The system of ordinary differential equations governing these processes was solved using an implicit integration solver, while species transport was coupled with a second-order explicit Runge-Kutta scheme to ensure numerical stability and accuracy.

The multiphase CFD model is described as follows:

The mass conservation equation for each phase *i* is given by

$$\frac{\partial}{\partial t}(\alpha_i \rho_i) + \nabla \cdot (\alpha_i \rho_i \boldsymbol{V}_i) = 0 \qquad (13)$$

and the momentum equation for each phase i is given by

$$\frac{\partial}{\partial t}(\alpha_i \rho_i \boldsymbol{V}_i) + \nabla \cdot (\alpha_i \rho_i \boldsymbol{V}_i \boldsymbol{V}_i) = -\alpha_i \nabla \mathrm{P} + \alpha_i \rho_i \boldsymbol{g} + \nabla \cdot (\alpha_i \bar{R}_i) + \boldsymbol{F}_i \qquad (14)$$

where ρ_i is the density, V_i is the phase velocity, P is the mean pressure, $\bar{R}_i$ is the combined viscous and Reynolds stresses for phase i; and F_i is the interface momentum transfer term, which is the sum of all the interfacial forces (lift, drag, virtual mass, wall lubrication, turbulent-dispersion forces, etc) acting on phase I from the other phase. It is noted that this term will influence bubble rise velocity and has large effect on gas hold-up calculation.

The transport of chemical species is modelled with passive scalar in each phase ad is given by

$$\frac{\partial}{\partial t}\left(\alpha_i \rho_i \boldsymbol{Y}_{ij}\right) + \nabla \cdot \left(\alpha_i \rho_i \boldsymbol{Y}_{ij} \boldsymbol{V}_i\right) = \nabla \cdot \left(\alpha_i \rho_i \overline{D}_{ij} \nabla Y_{ij}\right) + \dot{R}_{ij}^{MT} \quad (15)$$

Here Y_{ij} represents the mass fraction of species j in phase i, $\overline{D}_{ij}$ is the total species diffusion coefficient including both molecular and turbulent diffusion, and $\dot{R}_{ij}^{MT}$ is the interface mass transfer term for species j in phase i.

The Higbie mass transfer equation is given by,

$$\mathrm{Sh} = 1.14\mathrm{Re}^{0.5}\mathrm{Sc}^{0.5} \quad (16)$$

where Re is Reynold number, Sc is the Schmidt number which was used to characterize the mass diffusion and convection processes.

3. Results and Discussions

3.1 C_2-C_6 metabolites production

The growth profiles of *C. carboxidivorans* sp. 624 in both PETC and RCM media at different cultivation temperatures of 25°C, 30°C, and 37°C, were investigated using either N_2 or CO_2/H_2 (20/80) gas substrates at a headspace pressure of 150 kPa (RCM medium in **Fig. 1**, PETC medium in **Fig. S1**). The optimal temperatures for *C. carboxidivorans* have been reported differently in previous literature. Some studies suggest optimal growth occurs between 37°C and 40°C (Liou et al., 2005). Other research indicates that lower temperatures promote the production of acetate and ethanol, as well as facilitate carbon chain elongation (Ramió-Pujol et al., 2015). However, in our study, the *C. carboxidivorans* sp. 624 generally prefers an optimal temperature of 25°C. Comparison of the C_2 metabolites production between N_2 and CO_2/H_2 (20/80) gas substrates (RCM medium in **Fig. 1**, PETC medium in **Fig. S1**) suggests

evidence of CO_2 assimilation via WLP which corroborates with previous work (Antonicelli et al., 2023).

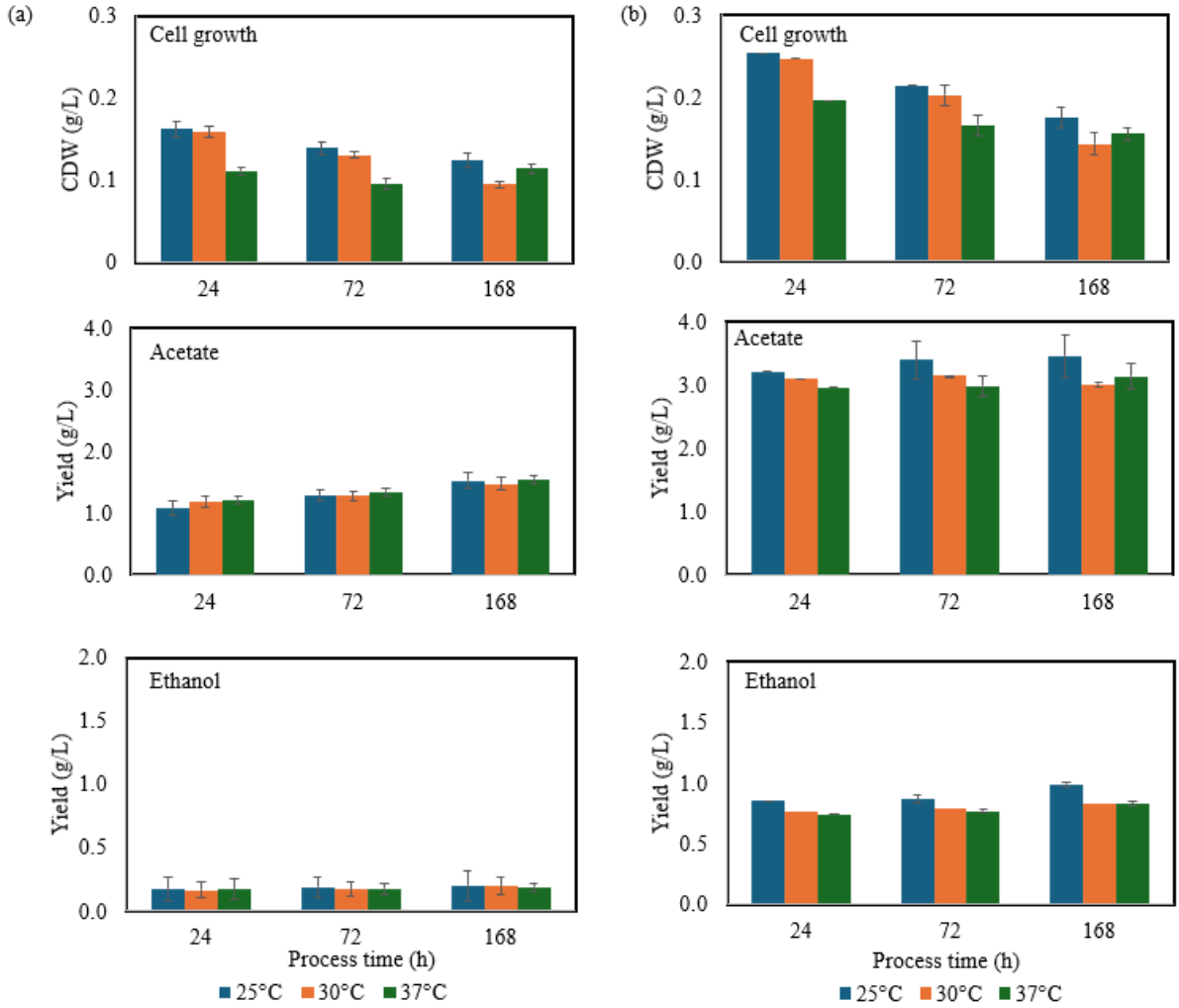

Fig. 1. Cell growth and production of C_2 metabolite analysis of *C. carboxidivorans* sp. 624 fermentation under **(a)** N_2, and **(b)** CO_2/H_2 (20/80) in RCM media at 25°C, 30°C, and 37°C.

To gain a deeper understanding of the metabolite production, detailed sampling of C_2-C_6 metabolites was conducted at 24, 48, 72, and 120 hours, in RCM media at 25°C under CO_2/H_2 (20/80) atmosphere (**Fig. 2** and **Fig. S2**). The CDW results (**Fig. 2a**) indicated that cell growth peaked by 24 hours (exponential phase) before gradually declining and ultimately reaching the stationary phase at 120 hours. This trend suggests that the initial cell proliferation

was primarily supported by organic nutrients in the media. Despite the decline in cell growth, continued metabolite accumulation beyond 24 hours implies sustained metabolic activity, driven by CO_2 assimilation via the WLP. This observation is consistent with findings by Antonicelli et al. (2023), who reported early exponential growth followed by a delayed cell growth increase beyond 10 days.

Among the acid metabolites production, acetate was the primary product during the exponential growth phase, reaching a notable yield of 2.17±0.22 g/L in RCM by 24 hours (**Fig. 2b**). Acetate yield continued to gradually increase, reaching 3.33 ± 0.21 g/L in RCM by 120 hours under CO_2/H_2 conditions, likely driven by sustained metabolic activity and carbon fixation. The higher acetate production in the presence of CO_2/H_2, relative to the N_2 control (1.08±0.09 g/L at 24 hours and 1.86±0.08 g/L at 120 hours, **Fig. 2b**) underscores the contribution of gas-phase CO_2/H_2 to acetate production. The slower rate of increase after 24 hours could be attributed to the inhibitory effects of accumulating byproducts, such as butanol, hexanoate, and hexanol (Oh et al., 2022). Similar trends for butyrate and hexanoate production were observed, where production was significant in the first 24 hours and slowed down after. Butyrate yield (**Fig. 2c**) remained relatively limited (<0.50 g/L) throughout the fermentation period, peaking at 0.41±0.06 g/L by 120 hours. Hexanoate production (**Fig. 2d**) followed similar trends to acetate, reaching an initial yield of 1.08±0.12 g/L within 24 hours and a final yield at 1.70±0.15 g/L by 120 hours. In terms of alcohols, their production remains minimal (<0.5 g/L) throughout the fermentation, indicating that solventogenesis pathway is not preferred under the investigated conditions (**Fig. S2**). Amongst which, ethanol is the most dominant solvent produced, compared butanol and hexanol (<0.1 g/L).

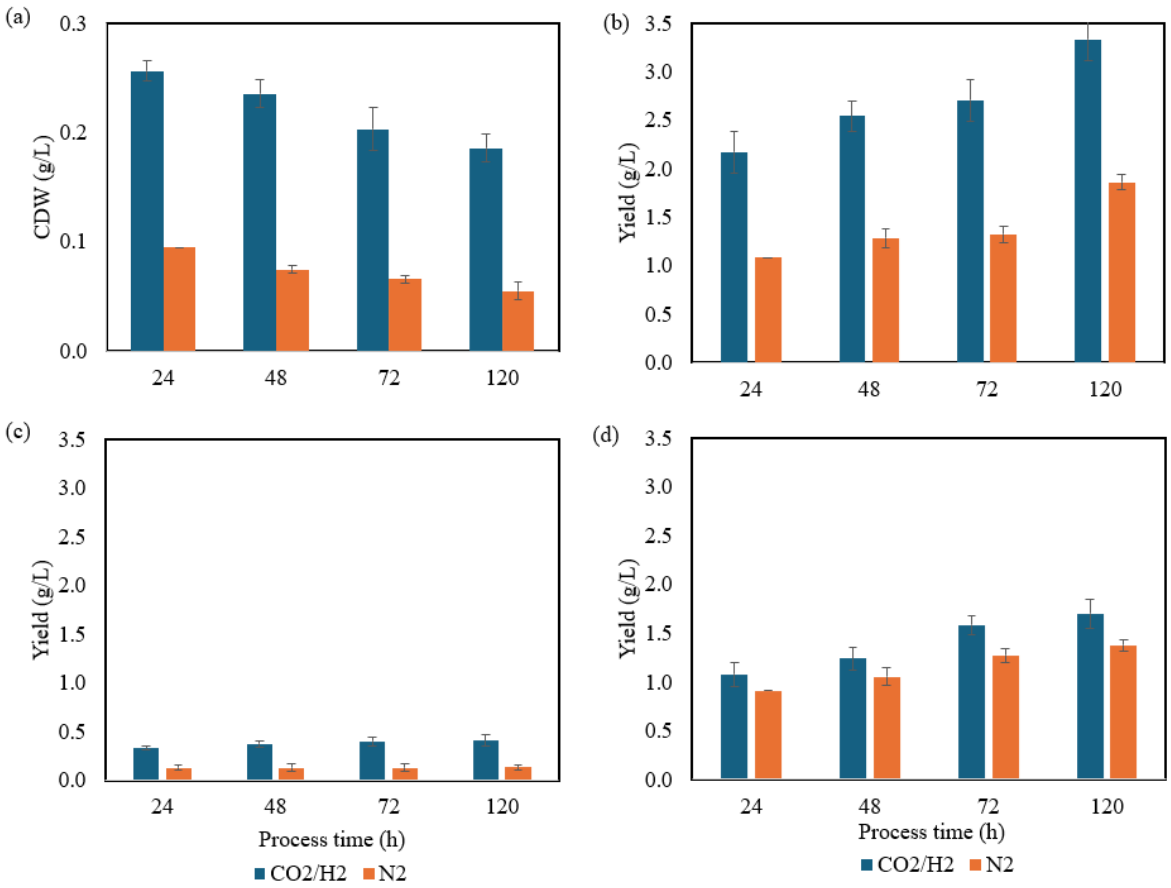

Fig. 2. *C. carboxidivorans* sp. 624 fermentation with CO_2/H_2 (20/80) or N_2 in RCM medium at 25°C: **(a)** Cell growth; Production yields of **(b)** Acetate, **(c)** Butyrate, and **(d)** Hexanoate.

3.2 Biokinetic model parameter estimation and experimental validation

The biokinetic model parameters (**Table S2**) were estimated by minimizing the root mean square error (RMSE) between predicted and experimental time-resolved metabolite concentrations. These parameters include the maximum biomass uptake rate for acid production, substrate affinity constants for biomass, maximum specific production rate of alcohols, substrate saturation constants, biomass decay rate, and yield coefficients. Due to the limitations of small-scale systems (e.g., serum bottles), where limited sample volume restricts the simultaneous measurement of substrate concentrations in both gas and dissolved phases, only metabolite profiles in liquid fermentation were used for model calibration. Initial

parameter estimates for chain elongation were derived from literature studies on C_2–C_6 acid production from CO_2/H_2 mixtures in membrane biofilm reactors (Chen and Ni, 2016).

The time-resolved metabolite concentration profiles obtained from 0D dynamic-kinetic model simulations, using the calibrated model parameters, were presented in **Fig. 3**. The simulated profiles exhibit good alignment with the experimental metabolite production over time, capturing key phases of gas fermentation, including biomass growth and decay, as well as the acetogenesis and solventogenesis processes. The RMSE value of 0.18 which falls within the acceptable range of <0.30 suggests reasonable accuracy of the model to predict experimental trends. Notably, the model successfully reproduced the maximum biomass concentration (0.25 g/L at ~24 hours) and the final yields of the C_2–C_6 acids and alcohols at 120 hours. This agreement suggests that the kinetic framework can capture the microbial metabolic shifts under CO_2/H_2 conditions. The ability to simulate both acidogenesis and solventogenesis further supports previous studies indicating that acetogens regulate electron flow to optimize carbon flux, with H_2 availability influencing the distribution of reduced products (Hermann et al., 2020; Zhu et al., 2020). Moreover, the model's predictive capability highlights the robustness of parameter estimation, ensuring reliable representation of the gas fermentation process across varying operating conditions. This is particularly relevant for process scale-up, where accurate kinetic modelling is essential for optimizing bioreactor performance and product selectivity (Singh et al., 2024).

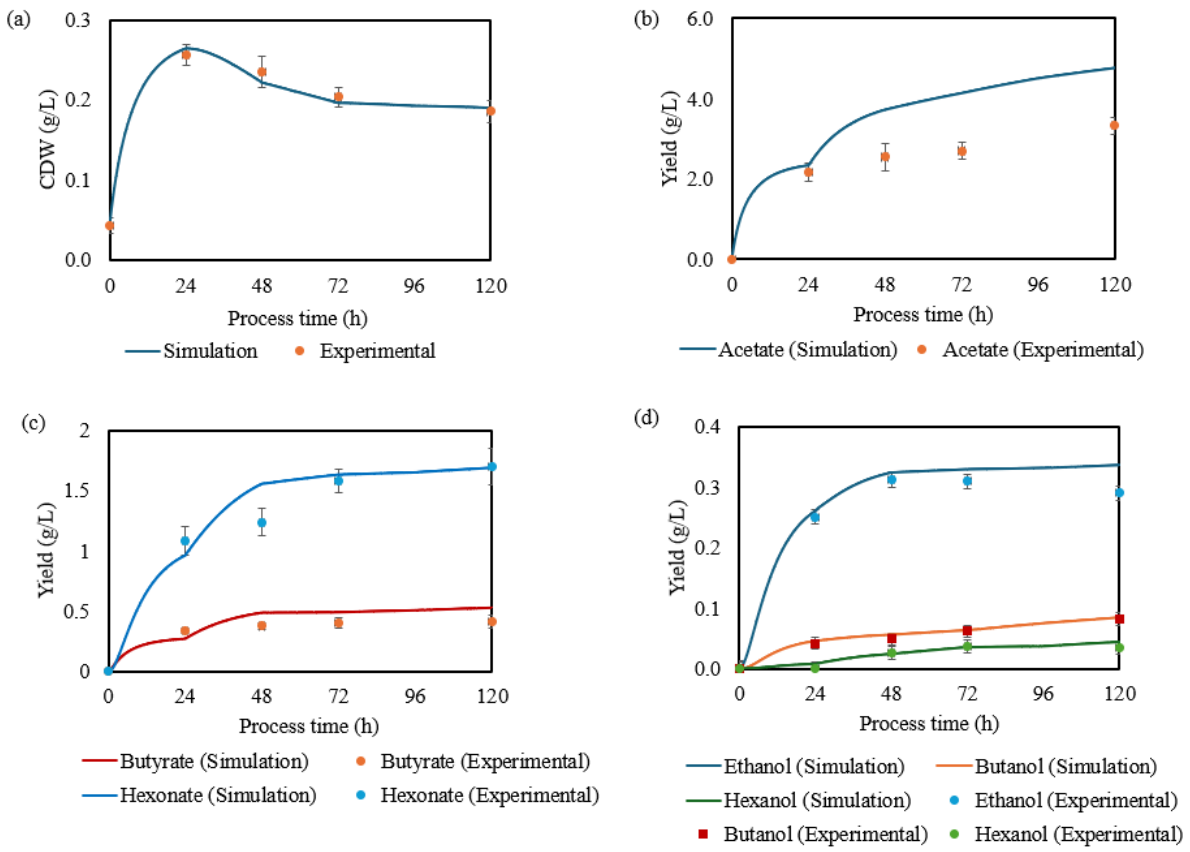

Fig. 3. Model predicted time-resolved profiles of bioconversion products along with experimental data: **(a)** Cell growth; Production yields of **(b)** acetate, **(c)** butyrate and hexanoate, as well as **(d)** ethanol, butanol and hexanol.

3.3 Effect of the liquid-to-gas volume ratio (V_L/V_G) on metabolite formation

The computational model was further applied to investigate the effect of the liquid-to-gas volume ratio (V_L/V_G) on metabolite formation, providing quantitative insights into biomass growth, dissolved H_2 concentration and metabolite distribution. Simulated total acid and alcohol concentrations at 24, 48, and 72 hours revealed that increasing the liquid volume enhances metabolite production, as presented in **Fig. 4a**. These model predictions were further validated by experimental fermentation under CO_2/H_2 gas conditions (**Fig. 4b**). Biomass growth followed a similar trend to product formation (**Fig. S3a**), increasing with higher V_L/V_G, suggesting that larger liquid volumes improve gas solubility and substrate availability, thereby

enhancing microbial metabolism. The larger liquid phase improves mass transfer rates by increasing the contact area between gas and liquid, reducing diffusion limitations (Lanzillo et al., 2020). The dissolved H_2 concentration profiles showed a gradual decline over time, with the lowest concentration at V_L/V_G = 0.25 and the highest at V_L/V_G = 4 (**Fig. S3b**). This trend emphasize the importance of liquid volume in stabilizing gas uptake rates, as a larger liquid phase can buffer against rapid depletion of dissolved H_2 by acting as a reservoir, thereby sustaining microbial metabolism for extended periods (Rahimi et al., 2018). Conversely, in lower V_L/V_G conditions, H_2 diffusion may be insufficient to match microbial consumption rates, leading to premature depletion and suboptimal metabolic activity (Ruggiero et al., 2022). These findings highlight the importance of gas-liquid mass transfer, where a larger liquid phase facilitates better substrate diffusion, ultimately boosting metabolic efficiency.

Unsurprisingly, the total acids and alcohols, as well as the acid-to-alcohol ratio, were strongly influenced by the H_2/CO_2 feedstock ratio (80:20) and the WLP (**Fig. 4b**). At 72 hours, V_L/V_G = 4 conditions yielded the highest total acids (5.34 g/L) and alcohols (0.41 g/L), highlighting the role of an H_2-rich environment in enhancing acetogenesis and chain elongation. The slightly lower acid-to-alcohol ratio (13) at V_L/V_G = 4 conditions indicates higher acid conversion to alcohols, supporting the hypothesis of product diversification through excess hydrogenation. Conversely, at V_L/V_G = 1, the fermentation produced the highest acid-to-alcohol ratio (18), favouring acetate production as moderate H_2 availability promoted acetogenesis while minimizing solventogenesis. Collectively, these findings demonstrate the interplay between gas-liquid interactions, substrate availability, and metabolic pathways in CO_2/H_2 fermentation. The computational model provides predictive insights that align with experimental observations, reinforcing the significance of optimizing V_L/V_G and electron donor-to-acceptor ratios to tailor product distribution in CO_2-based bioprocesses.

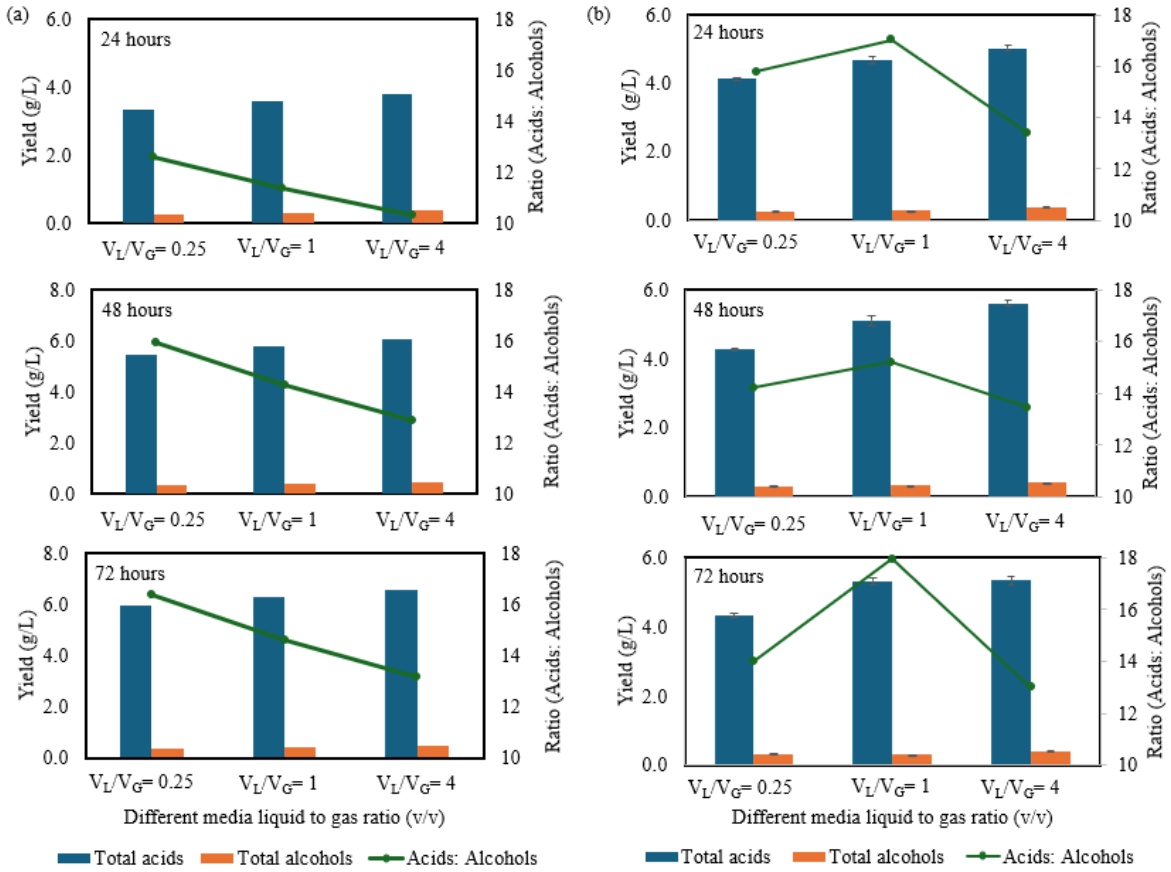

Fig. 4. Total acid and alcohol yields, and the corresponding acid-to-alcohol ratios at 24, 48, and 72 hours based on **(a)** Simulation, and **(b)** Experimental results from *C. carboxidivorans* sp. 624 fermentation using CO_2/H_2 (20/80) in RCM medium at 25 °C.

3.4 CFD simulations and validation

As we observed the impact of gas-liquid interactions, the importance of spatial distribution becomes more pronounced. A detailed understanding of the non-uniform spatial distributions of key components, such as substrates and metabolites, is essential, as these factors significantly impact cell growth and final bioproduction yields. To account for both temporal variations and spatial distributions within the bioreactor, the biokinetic model's estimated parameters were integrated with computational fluid dynamics (CFD) simulations. In small-scale batch systems, like serum bottles agitated at 200 rpm in this study, spatial variations and convective mixing effects are predicted to be minimal (Zhang et al., 2010). This

results in a largely good qualitative and quantitative agreement between 0D dynamic-kinetic model estimations and CFD simulations (**Fig. 5**), where time-resolved concentration profiles of biomass and metabolites are compared.

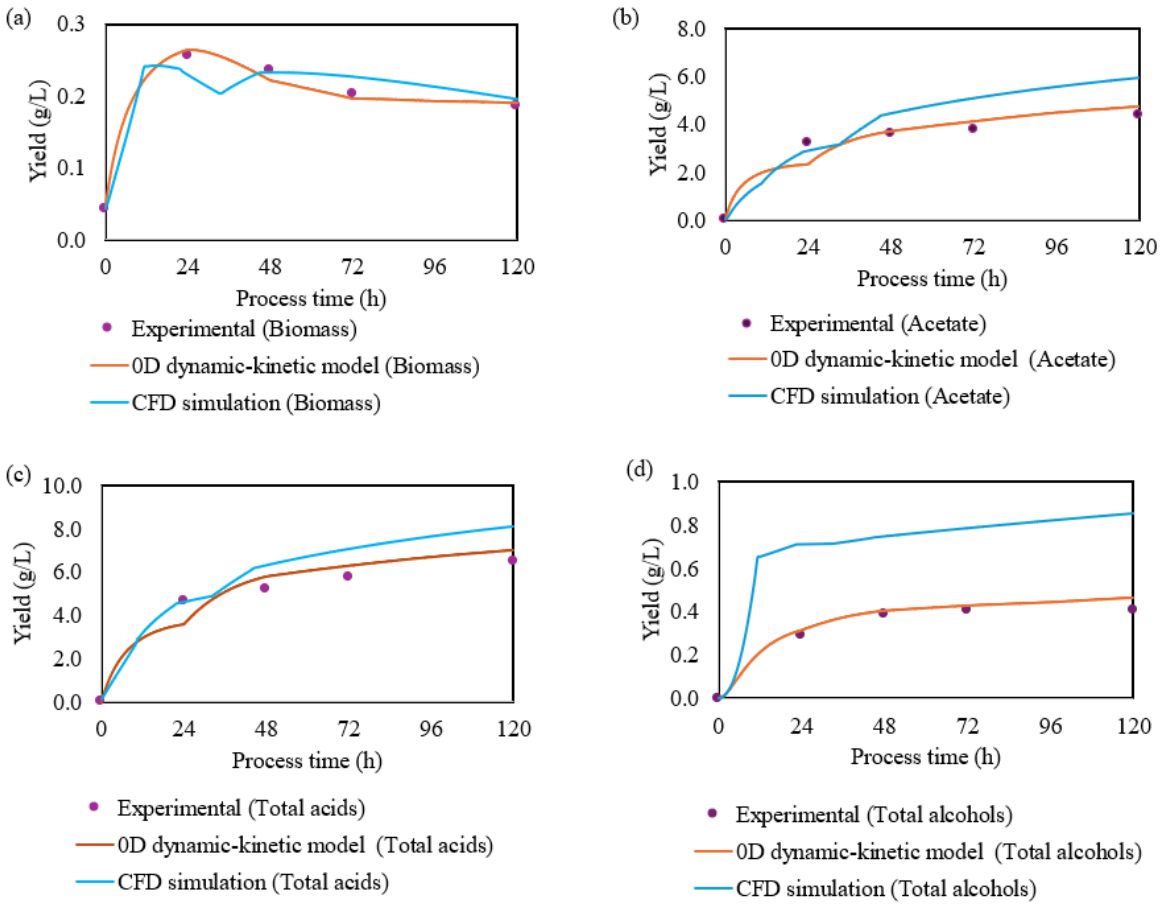

Fig. 5. Profiles calculated from 0D dynamic-kinetic model and integrated CFD simulations compared with experimental data (as in **Fig. 3**), **(a)** Cell growth (biomass), **(b)** Acetate, **(c)** Total acids, and **(d)** Total alcohols.

The concentration contours of biomass and acetate from 3D CFD simulations of the serum bottle model were analysed at different time points (5, 18, and 72 hours) during the *Clostridium carboxidivorans* sp. 624 fermentation under CO_2/H_2 (20/80) in RCM media (**Fig. 6a**). Simulations indicated a rise in biomass concentration from 5 to 18 hours (**Fig. 6b**).

Although acetate is later converted into ethanol, its sustained accumulation suggests its role as a key intermediate in the fermentation process. The spatial distribution patterns of biomass and acetate closely mirrored each other, indicating that acetate biosynthesis is linked to microbial growth, with active metabolism facilitating continuous acetate generation (Kurt et al., 2023).

At 5 hours, acids production dominates while alcohol levels are negligible, indicating the early acetogenic phase in the time-resolved concentration profiles (**Fig. 6c**). By 18 hours, acid production significantly exceeds that of alcohols, confirming the predominance of acetogenesis over solventogenesis. At 72 hours, both acids and alcohols production reach their maximum level, reflecting the transition to solventogenesis as more reducing equivalents become available for alcohol formation (**Fig. 6d**). The temporal distinction between metabolic phases corroborates with previous studies on syngas fermentation, where an extended acetogenic phase precedes solventogenesis under excess H_2 conditions (Lanzillo et al., 2020).

Overall, these results highlight the potential of CFD simulations to support gas fermentation process development. Factors such as spatial heterogeneities in substrate distribution, gas-liquid mass transfer, and hydrodynamics that crucially influence bioprocess efficiency can be captured in the model. It is worth acknowledging that application of serum bottle scale model may be limited as larger scale continuous stirred-tank reactors (CSTRs) undergo higher stirring frequencies and amplitudes. In CSTRs, physical and mechanical non-uniformities are more evident which could lead to greater discrepancies between CFD predictions and traditional 0D first-principles approaches (Hanspal et al., 2023). In larger bioreactors, factors such as mixing intensity, bubble dynamics, and localized nutrient gradients can lead to non-uniform microbial activity, potentially limiting productivity (Singh et al., 2024). Future research will expand therefore these simulations to pilot-scale systems to gain

deeper insights into fluid flow behaviour, optimize gas-to-liquid transfer efficiency, and refine operational strategies for improved metabolite yields in industrial applications.

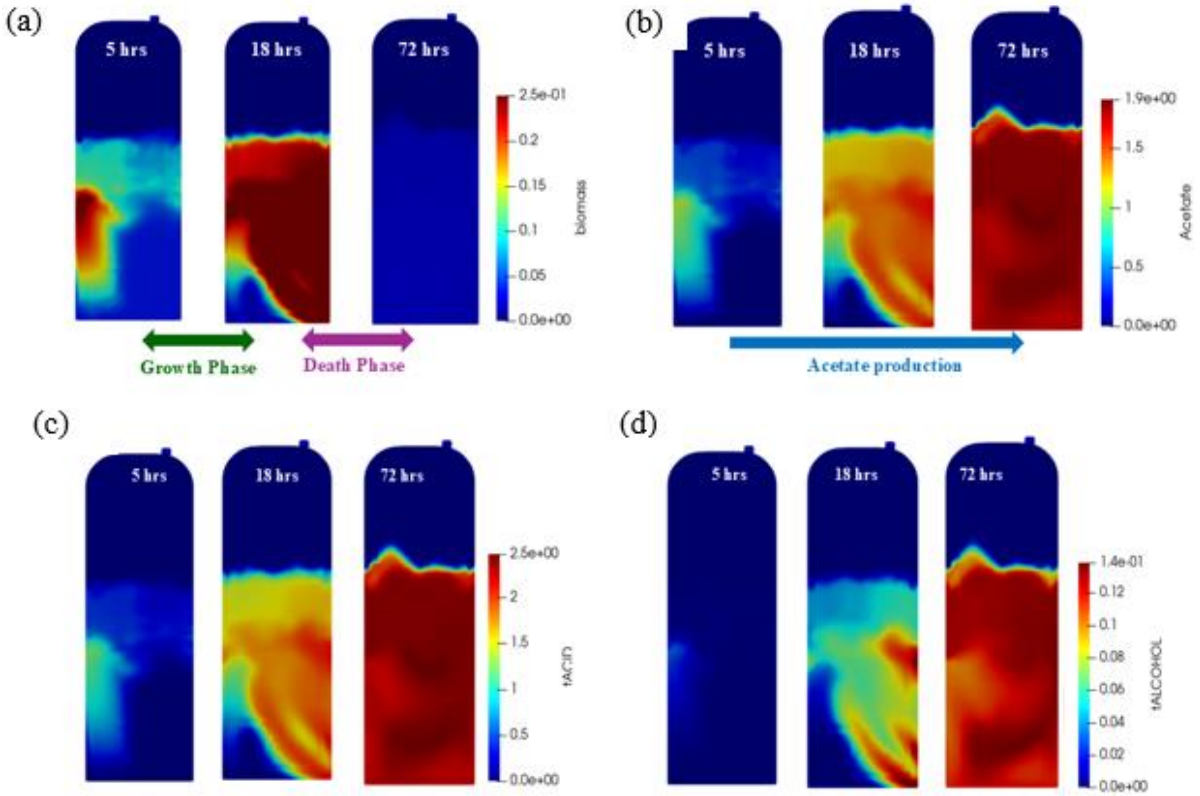

Fig. 6. Concentration contours at different time points of reaction **(a)** Cell growth (biomass), and **(b)** Acetate, **(c)** Total acids, and **(d)** Total alcohols.

4. Conclusion

This study demonstrates the potential of *Clostridium carboxidivorans* sp. 624 for CO_2/H_2 assimilation using a hybrid experimental and *in silico* and approach. A significantly higher acetate (3.33 g/L) and hexanoate (1.70 g/L) yields under CO_2/H_2 in RCM conditions, relative to the N_2 control, alludes to the role of gas-phase substrates in driving acetogenesis. The kinetic model and experimental validation highlight the crucial importance of the high liquid-to-gas volume ratio (V_L/V_G) and gas interactions in enhancing metabolite production and microbial metabolism during CO_2/H_2 fermentation. Integrated kinetic modelling and 3D

CFD simulations also informed bioprocess design for advancing scalable, carbon-negative CO_2 biomanufacturing.

Acknowledgements

The authors gratefully acknowledge financial support from Agency for Science, Technology and Research (A*STAR), Singapore (C233017002 and Singapore Integrative Biosystems and Engineering Research Strategic Research & Translational Thrust (SIBER SRTT). The computational work for this article was partially performed on resources of the National Supercomputing Centre (NSCC), Singapore (https://www.nscc.sg).

References

1. Acuña, P., Rebecchi, S., Vlaeminck, E., Quataert, K., Frilund, C., Laatikainen-luntama, J., Hiltunen, I., Winter, K. De, Soetaert, W.K., 2024. Demonstrating Pilot-Scale Gas Fermentation for Acetate Production from Biomass-Derived Syngas Streams. Fermentation 10, 1–13.
2. Antonicelli, G., Ricci, L., Tarraran, L., Fraterrigo Garofalo, S., Re, A., Vasile, N.S., Verga, F., Pirri, C.F., Menin, B., Agostino, V., 2023. Expanding the product portfolio of carbon dioxide and hydrogen-based gas fermentation with an evolved strain of Clostridium carboxidivorans. Bioresource Technology 387.
3. Chen, X., Ni, B.J., 2016. Anaerobic conversion of hydrogen and carbon dioxide to fatty acids production in a membrane biofilm reactor: A modeling approach. Chemical Engineering Journal 306, 1092–1098.
4. Doll, K., Rückel, A., Kämpf, P., Wende, M., Weuster-Botz, D., 2018. Two stirred-

tank bioreactors in series enable continuous production of alcohols from carbon monoxide with *Clostridium carboxidivorans*. Bioprocess and Biosystems Engineering 41, 1403–1416.

5. Dziejarski, B., Krzyżyńska, R., Andersson, K., 2023. Current status of carbon capture, utilization, and storage technologies in the global economy: A survey of technical assessment. Fuel 342.

6. Fernández-Naveira, Á., Veiga, M.C., Kennes, C., 2019. Selective anaerobic fermentation of syngas into either C_2-C_6 organic acids or ethanol and higher alcohols. Bioresource Technology 280, 387–395.

7. Hanspal, N., DeVincentis, B., Thomas, J.A., 2023. Modeling multiphase fluid flow, mass transfer, and chemical reactions in bioreactors using large-eddy simulation. Engineering in Life Sciences 23, 1–15.

8. Heffernan, J.K., Valgepea, K., de Souza Pinto Lemgruber, R., Casini, I., Plan, M., Tappel, R., Simpson, S.D., Köpke, M., Nielsen, L.K., Marcellin, E., 2020. Enhancing CO_2-Valorization Using Clostridium autoethanogenum for Sustainable Fuel and Chemicals Production. Frontiers in Bioengineering and Biotechnology 8, 1–10.

9. Hermann, M., Teleki, A., Weitz, S., Niess, A., Freund, A., Bengelsdorf, F.R., Takors, R., 2020. Electron availability in CO_2, CO and H_2 mixtures constrains flux distribution, energy management and product formation in *Clostridium ljungdahlii*. Microbial Biotechnology 13, 1831–1846.

10. Kurt, E., Qin, J., Williams, A., Zhao, Y., Xie, D., 2023. Perspectives for Using CO_2 as a Feedstock for Biomanufacturing of Fuels and Chemicals. Bioengineering 10, 1–41.

11. Lanzillo, F., Ruggiero, G., Raganati, F., Russo, M.E., Marzocchella, A., 2020. Batch syngas fermentation by clostridium carboxidivorans for production of acids and alcohols. Processes 8, 1–13.

12. Liew, F.M., Martin, M.E., Tappel, R.C., Heijstra, B.D., Mihalcea, C., Köpke, M., 2016. Gas Fermentation-A flexible platform for commercial scale production of low-carbon-fuels and chemicals from waste and renewable feedstocks. Frontiers in Microbiology 7, 694.

13. Liou, J.S.C., Balkwill, D.L., Drake, G.R., Tanner, R.S., 2005. *Clostridium carboxidivorans sp.* nov., a solvent-producing clostridium isolated from an agricultural settling lagoon, and reclassification of the acetogen *Clostridium scatologenes* strain SL1 as *Clostridium drakei sp.* nov. International Journal of Systematic and Evolutionary Microbiology 55, 2085–2091.

14. Manna, D., Chowdhury, R., Calay, R.K., Mustafa, M.Y., 2024. Experimental Insights into the Fermentation of Pyro-Syngas to Ethanol in a Semi-Batch and Continuous Stirred Bioreactor with Mathematical Modelling and Optimization. Energies 17 (3), 562.

15. Mariën, Q., Flores-Alsina, X., Aslam, U., Gernaey, K. V., Regueira, A., Ganigué, R., 2024. Isobutyric and n-butyric acid production from H_2 and CO_2 by *Clostridium luticellarii* in a hollow fiber membrane biofilm reactor: Reactor operation and process modelling. Chemical Engineering Journal 495, 153216.

16. Mast, Y., Wild, M., Takors, R., 2024. Optimizing Mass Transfer in Multiphase Fermentation: The Role of Drag Models and Physical Conditions. Processes 12.

17. Molitor, B., Mishra, A., Angenent, L.T., 2019. Power-to-protein: Converting renewable electric power and carbon dioxide into single cell protein with a two-stage bioprocess. Energy and Environmental Science 12, 3515–3521.

18. Ntagia, E., Chatzigiannidou, I., Carvajal-Arroyo, J.M., Arends, J.B.A., Rabaey, K., 2021. Continuous H_2/CO_2 fermentation for acetic acid production under transient and continuous sulfide inhibition. Chemosphere 285, 131536.

19. Oh, H.J., Ko, J.K., Gong, G., Lee, S.M., Um, Y., 2022. Production of Hexanol as the Main Product Through Syngas Fermentation by *Clostridium carboxidivorans* P7. Frontiers in Bioengineering and Biotechnology 10, 1–11.

20. Phillips, J.R., Atiyeh, H.K., Tanner, R.S., Torres, J.R., Saxena, J., Wilkins, M.R., Huhnke, R.L., 2015. Butanol and hexanol production in *Clostridium carboxidivorans* syngas fermentation: Medium development and culture techniques. Bioresource Technology 190, 114–121.

21. Puiman, L., Abrahamson, B., Lans, R.G.J.M. va. der, Haringa, C., Noorman, H.J., Picioreanu, C., 2022. Alleviating mass transfer limitations in industrial external-loop syngas-to-ethanol fermentation. Chemical Engineering Science 259, 117770.

22. Raganati, F., Ammendola, P., 2024. CO_2 Post-combustion Capture: A Critical Review of Current Technologies and Future Directions. Energy and Fuels, 38 (15).

23. Rahimi, M.J., Sitaraman, H., Humbird, D., Stickel, J.J., 2018. Computational fluid dynamics study of full-scale aerobic bioreactors: Evaluation of gas–liquid mass transfer, oxygen uptake, and dynamic oxygen distribution. Chemical Engineering Research and Design 139, 283–295.

24. Ramió-Pujol, S., Ganigué, R., Bañeras, L., Colprim, J., 2015. Incubation at 25°C prevents acid crash and enhances alcohol production in *Clostridium carboxidivorans* P7. Bioresource Technology 192, 296–303.

25. Ricci, L., Agostino, V., Fino, D., Re, A., 2021. Screening of gas substrate and medium effects on 2,3-butanediol production with *C. Ljungdahlii* and *C. autoethanogenum* aided by improved autotrophic cultivation technique. Fermentation *7*(4), 264.

26. Ruggiero, G., Lanzillo, F., Raganati, F., Russo, M.E., Salatino, P., Marzocchella, A., 2022. Bioreactor modelling for syngas fermentation: Kinetic characterization. Food

and Bioproducts Processing 134, 1–18.

27. Singh, V.K., Jiménez del Val, I., Glassey, J., Kavousi, F., 2024. Integration Approaches to Model Bioreactor Hydrodynamics and Cellular Kinetics for Advancing Bioprocess Optimisation. Bioengineering 11, 1–17.

28. Sun, X., Atiyeh, H.K., Huhnke, R.L., Tanner, R.S., 2019. Syngas fermentation process development for production of biofuels and chemicals: A review. Bioresource Technology Reports 7, 100279.

29. Thunuguntla, R., Atiyeh, H.K., Huhnke, R.L., Tanner, R.S., 2024. CO_2-based production of C_2-C_6 acids and alcohols: The potential of novel Clostridia. Bioresource Technology Reports 25, 101713.

30. Weller, H.G., Tabor, G., Jasak, H., Fureby, C., 1998. A tensorial approach to computational continuum mechanics using object-oriented techniques. Computers in Physics 12, 620–631.

31. Younesi, H., Najafpour, G., Mohamed, A.R., 2005. Ethanol and acetate production from synthesis gas via fermentation processes using anaerobic bacterium, *Clostridium ljungdahlii*. Biochemical Engineering Journal 27, 110–119.

32. Zhang, H., Williams-Dalson, W., Keshavarz-Moore, E., Shamlou, P.A., 2010. Computational-fluid-dynamics (CFD) analysis of mixing and gas–liquid mass transfer in shake flasks. Biotechnology and Applied Chemistry 41 (1), 1-8.

33. Zhu, H.F., Liu, Z.Y., Zhou, X., Yi, J.H., Lun, Z.M., Wang, S.N., Tang, W.Z., Li, F.L., 2020. Energy Conservation and Carbon Flux Distribution During Fermentation of CO or H_2/CO_2 by *Clostridium ljungdahlii*. Frontiers in Microbiology 11, 416.